Sensors and Materials, Vol. 35, No. 5 (2023) 1767–1773
MYU Tokyo

LETTER

S & M 3286

Colorimetric Dopamine Detection Based on Immobilized Monoamine Oxidase through Silver Nanoparticles

Gounhanul Shin,[1] Kunn Hadinoto,[2] and Jin-Won Park[1*]

[1]Department of Chemical and Biomolecular Engineering, College of Energy and Biotechnology,
Seoul National University of Science and Technology,
232 Gongneung-ro, Nowon-gu, Seoul 01811, Republic of Korea
[2]School of Chemical and Biomedical Engineering, Nanyang Technological University, Singapore 637459, Singapore

(Received February 20, 2023; accepted April 4, 2023)

Keywords: dopamine, monoamine oxidase, silver nanoparticles, oxidation

The colorimetric detection of dopamine was investigated to enhance the dopamine detection sensitivity. The detection was through the oxidation of AgNPs by hydrogen peroxide converted from dopamine along with dihydroxyphenylacetaldehyde. The conversion was facilitated by monoamine oxidase-Bs (MAO-Bs) bound to biomimetic membranes. The absorbance at 410 nm decreased with the increase in dopamine concentration. The limit of detection was determined to be 0.013 μM for 0.01 to 3.5 μM dopamine in the linear range of absorbance. The absorbance change corresponded to the conversion of Ag to Ag_2O, which occurred with the hydrogen peroxide released through MAO-Bs from dopamine. These results indicate that the AgNP degradation based on the immobilized MAO-Bs is sufficiently appropriate for the high-sensitivity absorbance detection of dopamine with a wide linear range.

1. Introduction

Dopamine (DA, a contraction of 3,4-dihydroxyphenethylamine), a brain neurotransmitter, has several distinct pathways, acting as a motivating factor of reward-motivated behavior and mediating movement control and hormone release.(1) Outside the central nervous system, DA is a paracrine messenger in the digestive system, immune system, kidneys, pancreas, and blood vessels, and is synthesized locally except in the blood vessels.(2) The major diseases of the nervous system are related to DA dysfunctions, and their medications work by altering the effects of DA.(3) Parkinson's disease progresses owing to the inability of neurons in the midbrain to secrete DA, which is widely treated with L-DOPA, a DA precursor. Schizophrenia is known to involve altered levels of DA activity, and its antipsychotic drugs are DA antagonists. Since attention deficit hyperactivity disorder (ADHD) is related to DA activity, dopaminergic stimulants are used to treat ADHD. DA is a medication manufactured for intravenous injection.

Therefore, technologies for DA quantification have been developed, including chromatography, mass spectrometry, optical spectroscopy, and electrochemical methods.(4–7) For

*Corresponding author: e-mail: jwpark@seoultech.ac.kr
https://doi.org/10.18494/SAM4356

ISSN 0914-4935
https://myukk.org/

analytical purposes, enzymes have been considered owing to their inherent selectivity under mild conditions. Monoamine oxidases (MAOs) are critical membrane proteins that catalyze oxidative deaminations.[8] MAOs are of two types, MAO-A and MAO-B, which have 70% structure similarity in the nervous system.[9] However, their distributions and functions are different. MAO-A is mostly found in the gastrointestinal tract, liver, placenta, and pulmonary vascular endothelium, whereas MAO-B is found in platelets.[10] Lipid layers, known as biomimetic membranes, are a platform for investigating the functions of biomolecules.[11–16] Previously, MAO was biomimetically reconstituted to detect DA using the electrochemical method with micromolar sensitivity.[17,18]

Metal nanoparticles have been intensively utilized owing to their unique electronic and optical properties, which occur through the interaction of the nanoparticles with light. The properties of AgNPs in solution are a yellow color and a strong absorption band around 400 nm.[19] Therefore, AgNPs were applied to detect various biomolecules such as metal ions, small molecules, proteins, DNA, and enzymes.[20–24] Dopamine detection was also considered in AgNP approaches.[25] In this work, we aimed to improve the sensitivity of dopamine detection using MAO-Bs immobilized in a lipid layer.

2. Materials and Methods

2.1 Monoamine oxidase immobilization

As a vessel for further assays, an eight-well cell culture slide was utilized. First, MAO-Bs were immobilized on the bottom surface inside each well of the slide. The surface was completely coated with 1.5% (w/v) octatrimethoxysilane (OTS) in 2 mL of anhydrous toluene for 1 h. The surface was sonicated in pure toluene for 20 min to remove nonbinding OTS molecules. The surface coated with OTS showed a contact angle of 100–105 degrees when a water drop was placed on the surface.

Chloroform was used to dissolve dioleoylphosphatidylcholine (DOPC) from Avanti and subsequently evaporated at room temperature under a nitrogen stream to form lipid films on the inside wall of a glass tube. The films were kept at a low pressure for 4 h to remove traces of the solvent and then hydrated overnight at room temperature in 5 mL of 10 mM 2-(*N*-morpholino) ethanesulfonic acid (MES) and 50 mM NaCl at pH 6.5. This hydration buffer either included MAO-Bs (1 U/mL) or not. The film-suspended solution was subjected to extrusion through two-stacked polycarbonate membranes of 100 nm pore size at room temperature to form uni-lamellar liposomes. The liposomes were also either embedded with MAO-Bs or not. The liposome solution was added to the surface coated with OTS to create a lipid layer.

2.2 Dopamine oxidation detection

To confirm that the MAO-Bs (1 U/mg, Sigma-Aldrich) bound to the lipid layer, the spectra obtained by X-ray photoelectron spectroscopy (PHI 5800, Physical Electronics, Inc., Chanhassen, MN) were utilized for each treatment, namely, the coating of OTS, the lipid layer formation of

DOPC liposomes only, and the lipid layer formation of MAO-B-bound DOPC liposomes. The concentrations of the added and unbound MAO-Bs were determined using the Bradford reagent. The surface density of the bound MAO-Bs was estimated to be about 3.4×10^{-3} ng-protein/mm^2-surface.

Both colorimetric assay and absorbance measurement were performed using AgNPs of 10 nm diameter (0.02 mg/mL solution, Sigma-Aldrich). The desired amount of dopamine was added inside the well, followed by the addition of 1.5 μL of AgNPs. Immediately after such additions, the color of the solution inside the cell was observed with the naked eyes. The absorbance was measured using a UV–Vis spectrometer (Shimazu, UV-1800). The changes in both color and absorbance were monitored with respect to the dopamine concentration (0, 0.01, 0.03, 0.08, 0.2, 0.5, 1.3, and 3.5 μM).

3. Results and Discussion

The intercalation of MAO-Bs was confirmed by XPS analysis, which was performed at each treatment, namely, OTS coating, lipid layer formation, and MAO-B-bound lipid layer formation. From the results of such analysis, the changes in the relative ratio of each element indicate the successful covalent attachment of MAO-Bs to the bottom surface inside each well of the slide, and the trend of the changes was consistent with those of the other enzymes published previously.[12,26,27] Prior to any treatment, the surface consisted only of silicon and oxygen (Table 1). After all of the treatments, the ratio of sulfur corresponding to the appearance of MAO-Bs was nonzero.

Different concentrations (0 to 3.5 μM) of dopamine solutions were evaluated to determine the sensitivity of the colorimetric assay 5 min after dopamine injection to reach equilibrium. The absorbance at 410 nm was monitored to determine the detection of dopamine. In other words, a yellow color and a high absorbance at 410 nm indicate the presence of AgNPs, whereas a pale color and a low absorbance indicate a degraded form from the nanoparticles. The color changes with the increase in dopamine concentration were observed as shown in Fig. 1. The injection into the lipid layer created with MAO-B-absent vesicles led little change in both color and absorbance.

The UV–Vis absorption spectra of solutions (Fig. 2) showed that the increase in dopamine concentration led to an absorbance decrease at 410 nm. The decrease reached the 3.5 μM concentration, which indicated the gradual degradation of the AgNPs. Although the increase at 300 nm due to the silver ion generation was observed, the change at 410 nm was more obvious.

Table 1
XPS results for each step of MAO-B immobilization.

Element	Glass slide (%)	OTS coating (%)	Lipid layer formation with DOPC liposomes (%)	Lipid layer formation with MAO-B-bound DOPC liposomes (%)
C 1s	0.1	28.5	27.9	26.8
N 1s	0.1	—	2.1	3.0
O 1s	66.5	49.0	47.9	47.6
Si 2p	33.3	23.5	22.1	21.5
S 2p	—	—	—	0.2

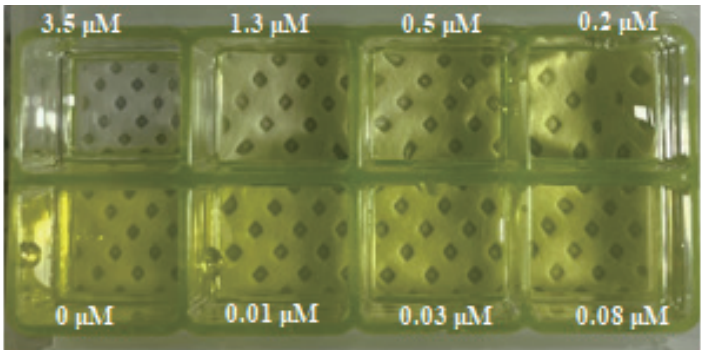

Fig. 1. (Color online) Color changes in AgNP solution with dopamine concentration.

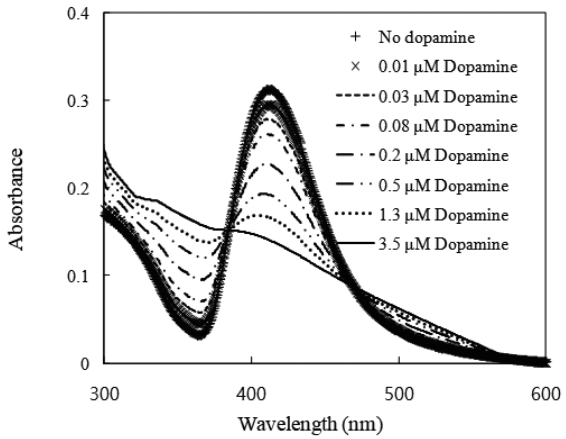

Fig. 2. UV–Vis absorption spectra of AgNP solution with dopamine concentration.

The limit of detection (*LOD*) was determined with the relation $LOD = 3.3\ \sigma/S$ in which σ is the standard deviation of four replicate responses and S is the slope of the curve (Fig. 3).[28] Hence, the *LOD* of dopamine obtained using the absorbance measurements was determined as 0.013 μM for the concentration range of 0.01 to 3.5 μM. These results indicate that the degradation of AgNPs is sufficiently appropriate for the absorbance detection of dopamine.

The detection mechanism is shown in Fig. 4. The good dispersion of AgNPs causes the yellow color. With the addition of dopamine, the oxidation of AgNPs was induced by the hydrogen peroxide converted from the dopamine along with dihydroxyphenylacetaldehyde. The conversion was facilitated by the MAO-Bs bound to the liposomes. Furthermore, the oxidation led to the formation of silver oxide (Ag_2O) that corresponded to the uncolored state. For the MAO-B-unbound liposomes, little change in the color and absorbance was observed. For the MAO-B-bound liposomes, the decrease in absorbance was proportional to the DA concentration.

Since enzymes have good specificity and high catalytic efficiency for sensing small molecular metabolites, several enzymes have been considered, including tyramine oxidase,

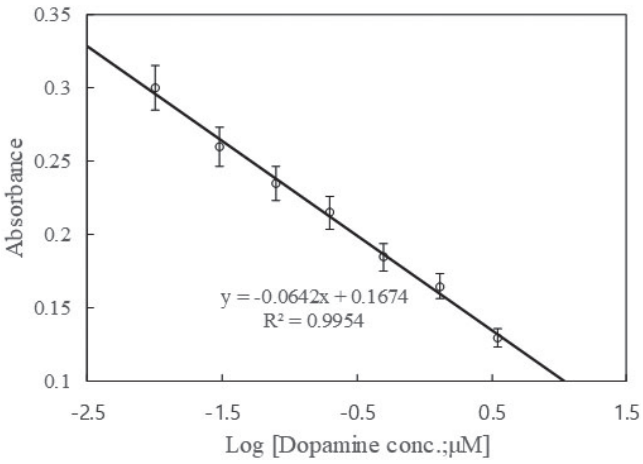

Fig. 3. Correlation between UV–Vis absorption and dopamine concentration.

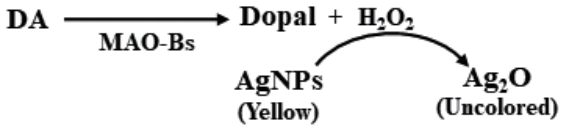

Fig. 4. Mechanism of dopamine detection in AgNP solution.

Table 2
Comparison of enzyme-based dopamine-sensing systems

	Optical sensor		Electrochemical sensor
	Fluorescence with carbon dots	This research	
LOD	0.03 μM	0.013 μM	20 μM
Linearity	0.1 to 6.0 μM	0.01 to 3.5 μM	50 to 250 μM
Sensitivity	2979.19 Abs./M	0.0642 Abs./log (μM)	0.095 μA/mM

horseradish peroxidase, and tyrosinase.[29–31] Not only the optical signal such as the absorbance but also the electrochemical signal was used to detect dopamine. The tyrosinase-based biosensors for dopamine are based on either a fluorescent or electrochemical signaling mechanism. The fluorescence of C_3N_4 was quenched by dopaminechrome produced through the tyrosinase-facilitated oxidation of dopamine, which was detected from 0.03 μM to 1 mM.[32] Similarly, the intensity of fluorescence with carbon dots decreased linearly with increasing dopamine concentration from 0.1 to 6.0 μM.[33] MAO-B-based electrochemical sensors show a lower *LOD*. Furthermore, compared with the optical signal, the electrochemical signal had an inherent limitation of narrow linear range.[18] In this research, the linear range was kept as an optical sensor and the higher *LOD* was suggested. The comparison is shown in Table 2. This comparison may be considered for the diagnosis of dopamine whose concentration is around 10–20 nM in a healthy condition.[34]

Besides dopamine, benzylamine and phenylethylamine can be oxidized by MAO-Bs.[35] Therefore, the methodology developed in this study has its own limitation to remove both amine derivatives prior to dopamine sensing.

4. Conclusions

In this study, the colorimetric detection of DA was investigated to achieve a higher sensitivity. The detection was through Ag oxidation facilitated by MAO-Bs bound to biomimetic membranes. The absorbance at 410 nm decreased with the increase in dopamine concentration. The detection limit was determined to be 0.013 μM for 0.01 to 3.5 μM dopamine in the linear range of absorbance. The absorbance change corresponded to the conversion of Ag to Ag_2O, which occurred with the hydrogen peroxide released through MAO-Bs from dopamine. These results indicate that the degradation of AgNPs is sufficiently appropriate for the high-sensitivity absorbance detection of dopamine with a wide linear range.

Acknowledgments

This study was supported by the Research Program funded by the SeoulTech (Seoul National University of Science and Technology).

References

1 K. C. Berridge: Psychopharmacology **191** (2007) 391. https://doi.org/10.1007/s00213-006-0578-x
2 R. A. Wise and M. J. Grubman: Annu. Rev. Psychol. **71** (2020) 79. https://doi.org/10.1146/annurev-psych-010418-103337
3 J. E. Carter, J. H. Johnson, and D. M. Baaske: Anal. Profiles Drug Subst. **11** (1982) 257. https://doi.org/10.1016/S0099-5428(08)60266-X
4 H. R. Kim, T.-H. Kim, S.-H. Hong, and H.-G. Kim: Biochem. Biophys. Res. Commun. **419** (2012) 632. https://doi.org/10.1016/j.bbrc.2012.02.064
5 H. Y. Wang, Y. Sun, and B. Tang: Talanta **57** (2002) 899. https://doi.org/10.1016/s0039-9140(02)00123-6
6 A. Kovac, Z. Somikova, N. Zilka, and M. Novak: Talanta **119** (2014) 284. https://doi.org/10.1016/j.talanta.2013.10.027
7 S. Qi, B. Zhao, H. Tang, and X. Jiang: Electrochim. Acta **161** (2015) 395. http://dx.doi.org/10.1016%2Fj.electacta.2015.02.116
8 E. E. Edmondson, A. Mattevi, C. Binda, M. Li, and F. Hubálek: Curr. Med. Chem. **11** (2004) 1983. https://doi.org/10.2174/0929867043364784
9 K. Chen, H. F. Wu, and J. C. Shih: J. Neurochem. **66** (1996) 797. https://doi.org/10.1046/j.1471-4159.1996.66020797.x
10 J. C. Shih amd K. Chen: Curr. Med. Chem. **11** (2004) 1995. https://doi.org/10.2174/0929867043364757
11 S.-R. Lee, Y. Park, and J.-W. Park: J. Biotechnol. **320** (2020) 77. https://doi.org/10.1016/j.jbiotec.2020.06.020
12 M. K. Kang and J.-W. Park: Sens. Mater. **33** (2021) 1749. https://doi.org/10.18494/SAM.2021.3408
13 Y. Park and J.-W. Park: Appl. Sci. **11** (2021) 3660. https://doi.org/10.3390/app11083660
14 G. Lee, K. Hadinoto, and J.-W. Park: Nanomaterials **12** (2022) 3683. https://doi.org/10.3390/nano12203683
15 M. K. Kang and J.-W. Park: J. Membr. Biol. **255** (2022) 55. https://doi.org/10.1007/s00232-021-00208-8
16 G. Lee and J.-W. Park: J. Korean Appl. Sci. Technol. **39** (2022) 720. https://doi.org/10.12925/jkocs.2022.39.5.720
17 C. M. Miyazaki, T. P. Pereira, D. B. T. Mascagni, M. L. de Moraes, and M. Ferreira: Mater. Sci. Eng. C **58** (2016) 310. https://doi.org/10.1016/j.msec.2015.08.042
18 P. Joshi, H. C. Joshi, S. K. Sanghi, and S. Kundu: Microchim. Acta **169** (2010) 383. http://ampri.csircentral.net/id/eprint/872

19 Y. A. Krutyakov, A. A. Kudrinskiy, A. Y. Olenin, and G. V. Lisichkin: Russ. Chem. Rev. **77** (2008) 233. http://dx.doi.org/10.1070/RC2008v077n03ABEH003751
20 S. Maiti, G. Barman, and J. K. Laha: Appl. Nanosci. **6** (2016) 529. https://doi.org/10.1007/s13204-015-0452-4
21 P. Wang, T. H. Wu, and Y. Zhang: Talanta **146** (2016) 175. https://doi.org/10.1016/j.talanta.2015.07.065
22 F. C. Marques, R. S. Alves, D. P. dos Santos, and G. F. S. Andrade: Phys. Chem. Chem. Phys. **24** (2022) 27449. https://doi.org/10.1039/D2CP03375E
23 Y. Wang, D. K. Xu, and H. Y. Chen: Lab Chip. **12** (2012) 3184. https://doi.org/10.1039/C2LC40322F
24 G. McConnell, S. Mabbott, A. L. Kanibolotsky, P. J. Skabara, D. Graham, G. A. Burley, and N. Laurand: Langmuir **34** (2019) 14766. https://doi.org/10.1021/acs.langmuir.8b01313
25 H. Wei, C. G. Chen, B. Y. Han, and E. K. Wang: Anal. Chem. **80** (2008) 7051. https://doi.org/10.1021/ac801144t
26 M. K. Kang and J.-W. Park: ACS Omega **6** (2021) 14963. https://doi.org/10.1021/acsomega.1c01023
27 M. K. Kang and J.-W. Park: Electron. J. Biotechnol. **52** (2021) 30. https://doi.org/10.1016/j.ejbt.2021.04.005
28 ICH Expert Working Group, Validation of Analytical Procedures: Text and Methodology. International Conference on Harmonization (ICH) Q2(R1) (2005) 11. https://database.ich.org/sites/default/files/Q2%28R1%29%20Guideline.pdf
29 H. Shinohara and F. Wang: Anal. Sci. **23** (2007) 81. https://doi.org/10.2116/analsci.23.81
30 P. Raghu, T. M. Reddy, P. Gopal, K. Reddaiah, and N. Y. Sreedhar: Enzyme Microb. Technol. **57** (2014) 8. https://doi.org/10.1016/j.enzmictec.2014.01.002
31 J. Njagi, M. M. Chernov, J. C. Leiter, and S. Andreescu: Anal. Chem. **82** (2010) 989. https://doi.org/10.1021/ac9022605
32 H. Li, M. M. Yang, J. Liu, Y. L. Zhang, Y. M. Yang, H. Huang, Y. Liu, and Z. H. Kang: Nanoscale **7** (2015) 12068. https://doi.org/10.1039/C5NR03316K
33 Z. D. Tang, K. Jiang, S. Sun, S. H. Qian, Y. H. Wang, and H. W. Lin: Analyst **144** (2019) 468. https://doi.org/10.1039/C8AN01659C
34 R. D. Badgaiyan: Prog. Brain Res. **211** (2014) 165. https://doi.org/10.1016/B978-0-444-63425-2.00007-6
35 H. Gaweska and P. F. Fitzpatrick: Biomol. Concepts **2** (2011) 365. https://doi.org/10.1515/BMC.2011.030

About the Authors

Gounhanul Shin is a senior undergraduate student at Seoul National University of Science and Technology. Her research interests are in biomimetic membranes. (sky000928@gmail.com)

Kunn Hadinoto received his B.S. degree from the University of Washington, USA, in 2000 and his Ph.D. degree from Purdue University, USA, in 2004. He joined NTU's School of Chemical & Biomedical Engineering as an assistant professor in 2007. Prior to that, he worked as a research fellow at the Agency of Science Technology & Research (A*STAR) Singapore. His research interests are in nanopharmaceuticals and their applications.
(KunnOng@ntu.edu.sg)

Jin-Won Park received his B.S. degree from Korea University, Korea, in 1998 and his M.S. and Ph.D. degrees from Purdue University, USA, in 2003 and 2005, respectively. From 2007 to 2010, he was an assistant professor at Gachon University, Korea. Since 2010, he has been a professor at Seoul National University of Science and Technology. His research interests are in biomimetic membranes and their applications. (jwpark@seoultech.ac.kr)